Ligand Effects

DOI: 10.1002/ange.201200689

The Origins of Dramatic Axial Ligand Effects: Closed-Shell $Mn^{V}O$ Complexes Use Exchange-Enhanced Open-Shell States to Mediate Efficient H Abstraction Reactions**

*Deepa Janardanan, Dandamudi Usharani, and Sason Shaik**

High-valent manganese-oxo complexes are currently in high demand because of their efficient catalysis of C–H bond activation,[1] their implications as intermediates during water splitting, for example in photosystem II,[2a] and their antioxidant activity.[2b,c] Many of these oxidation processes occur by an initial H-abstraction step. The efficient H-abstraction reactions with $Mn^{V}O$ reagents have been known to be mediated, not by the ground closed-shell states, but by the open-shell spin states wherein the metal-oxo moiety has an oxyl radical, Mn–O•, character,[3] and which generate the high-spin ground state of the $Mn^{IV}OH$.[1a,f] Indeed, having an oxyl radical is considered to be a pre-requisite for an efficient H abstraction[3b,c,4] by either a metal-oxo moiety or an oxide of a nonmetallic element, for example, P–O•. However, a recent report on the efficient H-abstraction reactivity by a series of $[(Cz)(X)Mn^{V}O]$ (Cz: corrolazinato^{3-}, X = none, F^-, CN^-) complexes, **1**–**3** in Scheme 1, appears to contrast this common view.[5] Complex **1** was diagnosed to possess a closed-shell singlet ground state,[5a] while **2** and **3** were assumed to have similarly closed-shell ground states,[5c] and nevertheless the latter two perform the H abstraction efficiently even though these states are not oxyl radicals. Moreover, the reaction series showed almost an unprecedented axial ligand effect, X^-. Thus, coordination of F^- was found to accelerate the reaction rate with dihydroanthracene (DHA) by a factor of 2100 relative to the pentacoordinate complex, and with CN^- as a ligand, the acceleration factor was 16000.[5c] These highly intriguing results are the focus of this work, which studies these reactions (Scheme 1) with an aim of answering the following fundamental questions: Considering that the ground state of the H-abstraction product, $[(Cz)(X)Mn^{IV}OH]$, is a quartet state ($S = 3/2$), can the closed-shell $[(Cz)(X)Mn^{V}O]$ states really function as the active oxidants in C–H activation from DHA? And, what are the reasons behind huge rate-enhancement attending the introduction of axial ligands?

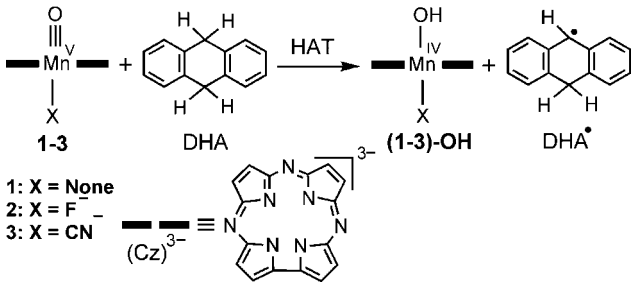

Scheme 1. Reactions investigated (HAT = hydrogen atom transfer).

These questions are addressed here by employing density functional theory (DFT) to characterize the oxidants and follow their reactions in Scheme 1. To this end, we used four different functionals starting with B3LYP, going through B3LYP* and B3LYP** which have decreasing percentages of Hartree–Fock exchange (20, 15, and 10%),[6] and ending with BP86 that has none. The results show that except for **1**, which unequivocally has a singlet ground state, **2** and **3** may have triplet ground states. However, irrespective of the spin-state identity in the ground state, the reaction itself is mediated by a specific triplet transition state that maximizes the exchange interactions, enjoys exchange-enhanced reactivity (EER),[7] has a large oxyl radical character as in other reactions of $Mn^{V}O$,[3b,c] and correlates directly to the quartet $Mn^{IV}OH$ product.

Following the same computational protocol as in a previous study,[5c] which simply overlooked the critical spin-state, the geometry optimization was carried out with UB3LYP using the LACVP basis set (B1). Energies were further refined using a larger LACV3P + * basis set (B2) incorporating solvent effects ($\varepsilon = 5.7$ and probe radius 2.72 Å corresponding to chlorobenzene) using the Poisson–Boltzmann solver in Jaguar 7.6.[8a] The B2 energies were augmented with thermal corrections from G03[8b] frequency calculations (see the Supporting Information for full details). B3LYP*, B3LYP**, and BP86 energies were determined by single-point calculations using B2 and solvent correction.

Figure 1a shows the optimized geometry of oxidant **1** in the three lowest states, the singlet state $S = 0$, and two triplet states S_A (S_B) = 1, while Figure 1b shows the orbital occupancy in $S = 0$. It is seen that **1** is characterized by a singlet ground state, $\delta^2 a_{1u}^{\ 2}$, with two triplet states lying above; one $S_A = 1$ having a $\delta^2\pi^{*1}a_{1u}^{\ 1}$ occupancy, and the other $S_B = 1$ with $\delta^1\pi^{*1}a_{1u}^{\ 2}$ occupancy. This state ordering is conserved in all the four functionals used by us (see Tables S1–S4 in the Supporting Information), and as such we feel safe to unequivocally

[*] Dr. D. Janardanan, Dr. D. Usharani, Prof. Dr. S. Shaik
Institute of Chemistry and The Lise Meitner-Minerva Center for Computational Quantum Chemistry, The Hebrew University Jerusalem, 91904 (Israel)
E-mail: sason@yfaat.ch.huji.ac.il

[**] Support by Minerva is thanked. Prof. H. Schwarz is thanked for pointing out the closed–open issue and reading the paper.

Supporting information for this article is available on the WWW under http://dx.doi.org/10.1002/anie.201200689.

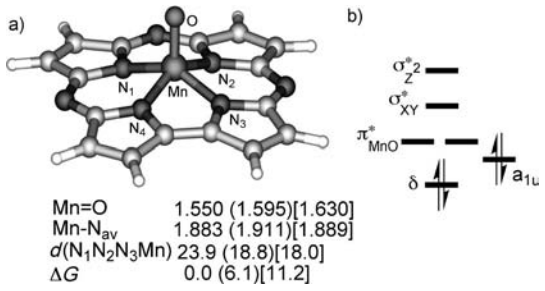

Figure 1. a) B3LYP key geometrical parameters (distances in Å, angles in °) and relative free energies (in kcal mol^{-1}) for **1**, given in the order $S=0$ ($S_A=1$)[$S_B=1$]. b) Orbital occupancy diagram for the $S=0$ state. $S_A=1$ has $\delta^2\pi^{*1}a_{1u}{}^1$ while $S_B=1$ has $\delta^1\pi^{*1}a_{1u}{}^2$.

assign the ground state of **1** as a singlet state, in agreement with experiment.[5a,c] Using the same strategy for **2** and **3**, we find that B3LYP and B3LYP* predict that the triplet state B is the ground state lying, respectively, 7 and 1 kcal mol^{-1} below the singlet state, whereas B3LYP** and BP86, which has a bias for low-spin states,[9] predict singlet ground states for both complexes. Since the experiment[5c] was unable to determine the spin state of these complexes, this issue remains as a challenge also for the experiment.

Quite different from the relative energy trends exhibited by the oxidants **1**–**3**, Figure 2 shows that the lowest transition-state species for the H-abstraction processes with DHA, is ^{3}**TS**$_{H,B}$ that is nascent from the triplet state B, irrespective of the ground state of the oxidant. Figure 2a shows the generic energy profile for **1** reacting with DHA, which in all the functionals has the same spin-state ordering of the energy profiles. The same ordering, as in Figure 2a, is obtained with B3LYP** for **2** and **3** reacting with DHA. Thus, assuming efficient spin-cross over prior to, or en route to H-transfer event,[7c,10] the reaction will be mediated by ^{3}**TS**$_{H,B}$ and proceeds directly to the ground state of the Mn^{IV}OH complex.[1a,3] Our calculations for **1**+DHA show that the minimum energy crossing point[10] coincides precisely with the energy of ^{3}**TS**$_{H,B}$. On the other hand, Figure 2b displays the B3LYP state orderings for the reactions of **2** and **3** (see also Figures S2–S4 in the Supporting Information), where triplet state B is the lowest profile throughout. Accordingly, whether the triplet state B is an excited state or a ground state, the H-abstraction reaction is unequivocally mediated by ^{3}**TS**$_{H,B}$

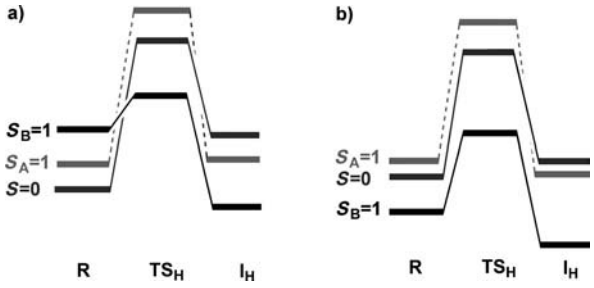

Figure 2. Generic state ordering for H-abstraction reactivity of **1**–**3** with DHA; a) **1** (with B3LYP, B3LYP* and B3LYP**) and **2**, **3** with B3LYP** b) **2**–**3** with B3LYP. **R** denotes the separate reactants, **TS**$_H$, the transition state, and **I**$_H$, the intermediate for H-abstraction step.

associated with this triplet state. BP86 yields the same trend for **2** and **3** as in Figure 2a, while for **1**, it predicts degenerate ^{1}**TS**$_H$ and ^{3}**TS**$_{H,B}$. Once again, the uniform showing that ^{3}**TS**$_{H,B}$ is the lowest transition state for **2** and **3**, and most likely also for **1**, and the respective intermediate that is uniformly nascent from triplet B; all these enable us to confidently single out this triplet state as the reactive state.

The root cause for the key role of the triplet state B will soon be elucidated, but before doing so let us inspect the B3LYP free-energy barriers in Table 1. Much like in the heme

Table 1: B3LYP free-energy barriers ($\Delta G^{\neq}_H$) and reaction energies (ΔG_{RI}) for the H abstraction from DHA by oxidants **1**–**3**.[a]

	$\Delta G^{\neq}_H/\Delta G_{RI}$ [kcal mol^{-1}]		
	1 (X=None)	**2** (X=F$^-$)	**3** (X=CN$^-$)
^{1}**TS**$_H$	31.7/16.5	30.3/4.5	29.2/5.4
^{3}**TS**$_{H,A}$	34.5/14.0	32.4/5.4	36.9/4.3
^{3}**TS**$_{H,B}$	23.0/−4.6	15.8/−14.7	14.4/−13.9

[a] Barriers ($\Delta G^{\neq}_H$) and reaction energies (ΔG_{RI}), including solvation corrections, are relative to the lowest state of the separated reactants; ^{1}**R** for **1** and ^{3}**R**$_B$ for **2** and **3**.

system,[3a–c] here too, the singlet state has very high barriers, and so are the barriers for the triplet state A. Additionally, the trends in the barriers (obtained from the lowest state of **R**) for the latter two states do not reflect much of the experimental trend, especially not the dramatic axial ligand effect. The good fit reported before[5c] for the singlet state is fortuitous, since it overlooked the ground states for **2** and **3**. The triplet state B features the lowest barriers, which also reproduce the observed significant axial ligand effect, showing a decrease of 7.2–8.6 kcal mol^{-1} in the barrier as the manganese ion gets ligated by F$^-$ and CN$^-$. The trends in the barriers of triplet state B follow the Bell–Evans–Polanyi effect,[11] and the exothermic nature of all the reactions accounts for the hydrogen atom transfer (HAT) efficiency of the oxidants.

Figure 3 shows the calculated free-energy barriers for the three different functionals, plotted against the experimental[5c] values. It is seen that irrespective of the functional (and hence

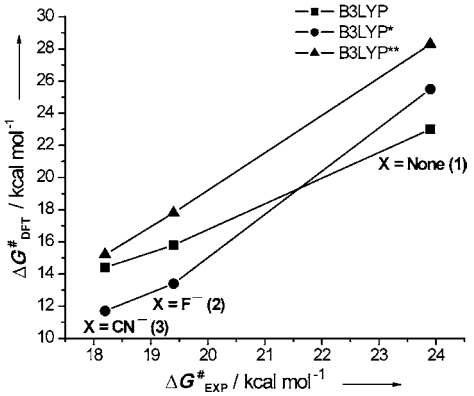

Figure 3. Correlation between experimental and computed free energy barriers for the reactions of **1**–**3** with DHA, in three different functionals.

also of the identity of the ground state), the trends in the barrier follows the experimental observation, and reproduces the observed very pronounced axial ligand effect on reactivity.

Another agreement with experiment[5c] is the kinetic isotope effect (KIE) values for **2** and **3**; the theoretical values for the reaction passing through ^{3}**TS**$_{H,B}$ are 8.2 and 7.1 and the experimentally measured ones are 10.5 and 6.7, respectively. Therefore the overall theoretical agreement with experiment makes a solid case for the proposal that the triplet state B mediates the H abstraction. The support of a singlet-state reactivity based on the identity of the ground state is never certain.[12] Interestingly, the KIE value for the reactions of **2** and **3** are similar for the triplet and singlet states (8.2 and 7.1 for ^{3}**TS**$_{H,B}$ vs. 8.7 and 8.5 for ^{1}**TS**$_H$). By contrast, for oxidant **1** the calculated KIE value for the reaction proceeding via ^{3}**TS**$_{H,B}$ is very low (KIE(S_B=1) = 2.3), whereas for the corresponding singlet-state reaction, the value is high (KIE-(S=0) = 8.9). So here the calculations predict that if the reaction of **1** proceeds via the singlet-state TS, the KIE will be high, whereas if the reaction is mediated by the triplet state like those of **2** and **3**, the KIE will be rather low.

Let us discuss now the reactivity of the singlet state and triplet states A and B, and try to comprehend the preference of the latter state using the simplified orbital diagrams in Scheme 2 that follows the electronic reorganization during the H abstraction. Thus, as the H is being transferred, its electron shifts to an orbital in the [(Cz)(X)MnO] moiety, whereas the remaining proton makes an O–H bond with a lone pair on the oxo ligand, as in proton-coupled electron transfer (PCET) mechanisms.[7b,13] Thus, on the S = 0 surface, in Scheme 2a, a shift of an α electron from the σ_{CH} orbital of the substrate to the π* orbital of MnO leaves behind a β electron on the substrate φ_C orbital, and results in an open-shell singlet configuration in ^{1}**I**$_H$. The triplet A state (Scheme 2b), on the other hand, involves a shift of a β electron from σ_{CH} to fill the ligand a_{1u} orbital, leaving an

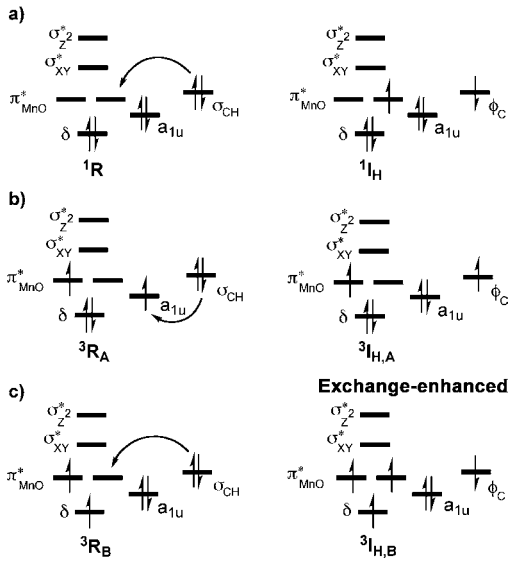

Scheme 2. Electron reorganization during H abstraction from DHA by **1**–**3** in: a) S = 0, b) S_A = 1, and c) S_B = 1 spin states.

α electron in the substrate φ_C orbital. Thus, ultimately, the S = 0 and the S_A = 1 states acquire the same electronic structure, with the difference being the spin orientation in φ_C. Consequently, the two TSs and the corresponding intermediate states will have closer energies. By contrast, in the S_B = 1 state (Scheme 2c), an α electron shifts from σ_{CH} to π*, and leaves a β electron in φ_C. As such, now the number of exchange interactions on the manganese center increases to three, thus leading to stabilization of ^{3}**TS**$_{H,B}$ on the triplet state B energy surface. Note also from Scheme 2c that the triplet B correlates directly to the intermediate which involves the S = 3/2 state of Mn^{IV}OH,[3b,c] which is the expected ground state of the Mn^{IV} complex.[1a,f]

Figure 4 displays the spin natural orbitals of ^{3}**TS**$_{H,B}$ and illustrates that, in fact, as described in Scheme 2c, the exchange enhancement for the triplet state B occurs already

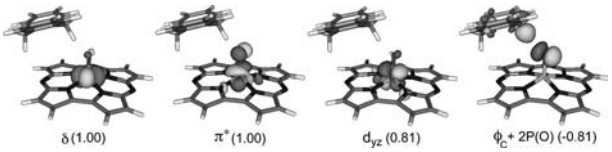

Figure 4. Spin natural orbitals and their occupations (noted in parentheses) in ^{3}**TS**$_{H,B}$ for the H-abstraction reaction of **1** with DHA. A negative occupation number means β spin. ^{3}**TS**$_{H,B}$ species for **2** and **3** have similar electronic structures.

in the transition state. It is seen that ^{3}**TS**$_{H,B}$ has already four approximately singly occupied spin orbitals, three of which are centered on Mn and/or on MnO, carry α spins, and the fourth (φ_C) which is shared between DHA and the O atom of MnO, carries a β spin (negative spin density). Thus, as the H is being abstracted in triplet state B, the Mn^V center in the TS becomes Mn^{IV} and is enriched by exchange relative to the other transition states. Indeed, the spin density distribution on Mn, ρ(Mn), shows that the ratio of [ρ(Mn);^{3}**TS**$_{H,B}$]/[ρ(Mn);^{1}**TS**$_H$] is 2.88 for **1**, 3.15 for **2**, and 2.93 for **3**; similar ratios are found for [ρ(Mn);^{3}**TS**$_{H,B}$]/[ρ(Mn);^{3}**TS**$_{H,A}$]. As discussed previously, this type of electronic reorganization that increases the number of exchange interactions on the metal can lead to exchange-enhanced reactivity (EER),[7b] which is so prevalent in oxidative processes by metal-oxo reagents.[7,13]

While the electronic structure of ^{3}**TS**$_{H,B}$ experiences exchange stabilization, we still have to account for the fact that it lies below both ^{1}**TS**$_H$ and ^{3}**TS**$_{H,A}$, irrespective of the functional used here to probe the reactivity (with the exception of BP86, which predicts that for **1** the transition states ^{1}**TS**$_H$ and ^{3}**TS**$_{H,B}$ are degenerate). Let us then consider the relative energy of ^{3}**TS**$_{H,B}$ relative to ^{1}**TS**$_H$ or ^{3}**TS**$_{H,A}$. Thus, as we argued before, ^{3}**TS**$_{H,B}$ is stabilized relative to ^{1}**TS**$_H$ or ^{3}**TS**$_{H,A}$ by three units of exchange interaction (3 K), but this exchange stabilization is opposed by the orbital excitation from δ to π* (ΔE_{excit}) that is needed to generate ^{3}**TS**$_{H,B}$ from ^{1}**TS**$_H$ or ^{3}**TS**$_{H,A}$. The relative energies of ^{3}**TS**$_{H,B}$ to ^{1}**TS**$_H$ or ^{3}**TS**$_{H,A}$ will therefore be determined approximately by the balance of these two terms, namely by ΔE_{excit} −3 K. These terms were estimated for ^{3}**TS**$_{H,B}$ and ^{1}**TS**$_H$, and are given in Table S14 in the Supporting Information. The K values

between d orbitals of transition metals are reduced roughly to around 50–70% of the atomic exchange because of orbital delocalization. Indeed, our exchange values for the oxidants are 11.1, 12.4, and 12.9 kcal mol^{-1} for **1**, **2**, and **3**, respectively, compared with 19.8 kcal mol^{-1} for Mn^{+}.[14] On the other hand, the ΔE_{excit} term evaluated from SCF energy differences (see Table S14 in the Supporting Information), are 26.4, 14.8, and 18.5 kcal mol^{-1}, for the three oxidants in the respective order. Carrying over these values to the respective transition states, one can derive the following conclusions: In the case of **1**, the 3 K stabilization is 33.3 kcal mol^{-1} which is larger than ΔE_{excit} (26.4 kcal mol^{-1}), thereby leading to a net stabilization of ^{3}**TS**$_{H,B}$ by 6.8 kcal mol^{-1} relative to ^{1}**TS**$_{H}$, in good agreement with 6.4 kcal mol^{-1}, which is the B3LYP computed energy difference between ^{1}**TS**$_{H}$ and ^{3}**TS**$_{H,B}$ (see in the Supporting Information Table S5, B2 + solv energies). Similar considerations lead to values of 22.4 and 20.1 kcal mol^{-1} stabilization energies of ^{3}**TS**$_{H,B}$ relative to ^{1}**TS**$_{H}$, for **2** and **3**, respectively, compared with the B3LYP computed values of 16.0 and 14.0 kcal mol^{-1}. These values predict that in all cases, the ^{3}**TS**$_{H,B}$ is the lowest energy transition state, and the computed trend in the ^{3}**TS**$_{H,B}$-^{1}**TS**$_{H}$ energy gaps for **1**–**3** follows the balance of exchange enhancement versus orbital excitation energies, showing a jump on moving from **1** to **2** and **3**. Thus, the dramatic axial ligand effect observed by experiment with **1**–**3** reacting with DHA,[5c] originates in the net stabilization of ^{3}**TS**$_{H,B}$ because of the EER of this state relative to the singlet TS. This EER stabilization exhibits a jump from 6.8 to 22.4 and 20.1 kcal mol^{-1}, after the axial ligands are introduced to the [(Cz)Mn^{V}O] complex, because of a combination of an increase of the 3 K term and a concomitant decrease of the ΔE_{excit}. It is important to note here that, in accord with previous expectations,[3a–c,4] the most reactive state $S_B = 1$ is also the one with the higher oxyl radical character, whereas $S = 0$ has no such character.

In accord with general reactivity patterns of other metal-oxo reagents,[7b] here too, as shown in Figure 5, the geometric features of the optimized transition states are in agreement with the nature of the electron shifts in Scheme 2. Thus, as shown in Scheme 2, the ^{1}**TS**$_{H}$ and ^{3}**TS**$_{H,B}$ are characterized by electron shift from the σ_{CH} orbital of DHA to the π^* orbital of MnO, and as such, these TSs assume a bent side-on trajectory

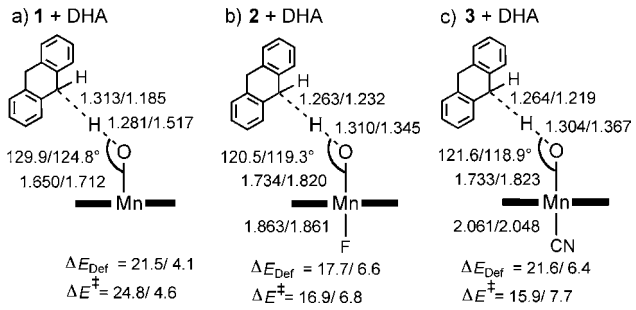

Figure 5. Key geometric details of ^{1}**TS**$_{H}$/^{3}**TS**$_{H,B}$ in **1**–**3**. Given underneath the TSs are the deformation energies (in kcal mol^{-1}) of the species and the corresponding electronic barriers (UB3LYP/B2 + solv// B1 in kcal mol^{-1}) relative to the separate reactants at a given spin state.

with Mn-O-H angles of around 120°.[7b] The higher barrier on the singlet-state surface is well-correlated with the total deformation energy in the TSs,[15] which for **1** is dominated by the degree of stretching of the C–H bond of the DHA, whereas for **2** and **3** the deformation of the oxidant moiety contributes more than 50% of the total deformation energy (Table S16 in the Supporting Information). Note that ^{3}**TS**$_{H,B}$ which features double occupancy of the π^* orbitals, possesses accordingly elongated Mn–O bonds in all the oxidants (Figure 5) but more so in **2** and **3**. This Mn–O bond elongation is the root cause of the reduced orbital excitation in **2** and **3** in ^{3}**TS**$_{H,B}$, and at the same time it increases the oxyl-radical character of these oxidants,[3b,c,4d] and contributes thereby to the superior reaction thermodynamics, thus enhancing their reactivity.[5c] All these features are manifestations of the EER, which establishes a lower ^{3}**TS**$_{H,B}$ with a small deformation energy of the reactants,[13b] while the ^{1}**TS**$_{H}$ species which is deprived of exchange enhancement has a high deformation energy, a less exothermic reaction, and a higher barrier.

An interesting example that follows the above trend, based on the EER principle,[7b] is the recent report that the analogous diamagnetic pentacoordinate oxomanganese(V)-corroles were found to be inert towards olefin epoxidation,[16a] whereas by contrast, the same reagents undergo stoichiometric oxygen atom transfer (OAT) reactions with phosphines[16a] and thioethers.[16b] OAT reactions are two-electron processes that respond to the electron accepting property of the oxidant (its electrophilicity)[17,18] and do not require exchange enhancement to proceed.[7b]

In conclusion, the computed barriers and kinetic isotope effects (KIEs) for the HAT reactions of [(Cz)(X)Mn^{V}O] complexes with DHA, reproduce the experimental trends[5c] and especially the dramatic axial ligand effect, whereby coordinating the manganese center with anionic and electron-rich ligands enhances the reactivity by more than four orders of magnitude.[18b] The present work reveals once again that the closed-shell state of the reagent is not the reactive state even if it is sometimes the ground state.[12] From the closed-shell state, which has no unpaired electrons initially, the oxyl radical is created en route to the transition states, and this requires a high deformation energy and a correspondingly high barrier. The reactive state in the [(Cz)(X)Mn^{V}O] complexes is the triplet state ($\delta^{1}\pi^{*1}$, Scheme 2b) that has a high oxyl radical character and is the state that enjoys exchange-enhanced reactivity (EER)[7] because of the increase in the number of exchange interactions in the respective transition state ^{3}**TS**$_{H,B}$ compared with the singlet-state TS. It is no wonder that this state dominates the reactivity on Mn^{V}O, since after all the H abstraction generates Mn^{IV}OH,[3b,c] which is known to possess a quartet ground state and is nascent from the triplet state B. Finally, the study predicts that for **1**, [(Cz)Mn^{V}O], which is devoid of the axial ligand, and clearly has a singlet ground state, that measurement of the KIE for the reaction of DHA can distinguish between a reaction mediated via ^{1}**TS**$_{H}$ (KIE = 8.9), and the one mediated via ^{3}**TS**$_{H,B}$ (KIE = 2.3). Since BP86 predicts closely lying transition states ^{1}**TS**$_{H}$ and ^{3}**TS**$_{H,B}$, such a test would be important to bridge experiment and theory on spin-state issues in reactivity.[19]

Received: January 25, 2012
Published online: March 21, 2012

Keywords: density functional calculations · exchange-enhanced reactivity · high-valent Mn–oxo · hydrogen atom abstraction

[1] a) The ground state of Mn^{IV} complexes is generally $S = 3/2$. See discussion in: R. S. Czernuszewicz, Y. O. Su, M. K. Stern, K. A. Macor, D. Kim, J. T. Groves, T. G. Spiro, *J. Am. Chem. Soc.* **1988**, *110*, 4158 – 4165; b) M. F. Ryan, A. Fiedler, D. Schröder, H. Schwarz, *J. Am. Chem. Soc.* **1995**, *117*, 2033 – 2040; c) N. Jin, J. T. Groves, *J. Am. Chem. Soc.* **1999**, *121*, 2923 – 2924; d) D. Balcells, C. Raynaud, R. H. Crabtree, O. Eisenstein, *Chem. Commun.* **2009**, 1772 – 1774; e) W. Liu, J. T. Groves, *J. Am. Chem. Soc.* **2010**, *132*, 12847 – 12849; f) X. Wu, M. S. Seo, K. M. Davis, Y.-M. Lee, J. Chen, K.-B. Cho, Y. N. Pushkar, W. Nam, *J. Am. Chem. Soc.* **2011**, *133*, 20088 – 20091.

[2] a) J. P. McEvoy, G. W. Brudvig, *Chem. Rev.* **2006**, *106*, 4455 – 4483; b) A. Mahammed, Z. Gross, *Angew. Chem.* **2006**, *118*, 6694 – 6697; *Angew. Chem. Int. Ed.* **2006**, *45*, 6544 – 6547; c) Z. Okun, L. Kupershmidt, T. Amit, S. Mandel, O. Bar-Am, M. B. H. Youdim, Z. Gross, *ACS Chem. Biol.* **2009**, *4*, 910 – 914.

[3] a) F. De Angelis, N. Jin, R. Car, J. T. Groves, *Inorg. Chem.* **2006**, *45*, 4268 – 4276; b) D. Balcells, C. Raynaud, R. H. Crabtree, O. Eisenstein, *Inorg. Chem.* **2008**, *47*, 10090 – 10099; c) D. Balcells, C. Raynaud, R. H. Crabtree, O. Eisenstein, *Chem. Commun.* **2008**, 744 – 746.

[4] a) N. Dietl, M. Engeser, H. Schwarz, *Angew. Chem.* **2009**, *121*, 4955 – 4957; *Angew. Chem. Int. Ed.* **2009**, *48*, 4861 – 4863; b) D. Schröder, J. Roithová, *Angew. Chem.* **2006**, *118*, 5835 – 5838; *Angew. Chem. Int. Ed.* **2006**, *45*, 5705 – 5708; c) E. I. Solomon, S. D. Wong, L. V. Liu, A. Becker, M. S. Chow, *Curr. Opin. Chem. Biol.* **2009**, *13*, 99 – 113; d) S. Ye, F. Neese, *Proc. Natl. Acad. Sci. USA* **2011**, *108*, 1228 – 1233; e) N. Dietl, M. Schlangen, H. Schwarz, *Angew. Chem.* **2012**, *124*, DOI: 10.1002/ange.201108363; *Angew. Chem. Int. Ed.* **2012**, *51*, DOI: 10.1002/anie.201108363.

[5] a) D. E. Lansky, B. Mandimutsira, B. Ramdhanie, M. Clausén, J. Penner-Hahn, S. A. Zvyagin, J. Telser, J. Krzystek, R. Q. Zhan, Z. P. Ou, K. M. Kadish, L. Zakharov, A. L. Rheingold, D. P. Goldberg, *Inorg. Chem.* **2005**, *44*, 4485 – 4498; b) D. E. Lansky, D. P. Goldberg, *Inorg. Chem.* **2006**, *45*, 5119 – 5125; c) K. A. Prokop, S. P. de Visser, D. P. Goldberg, *Angew. Chem.* **2010**, *122*, 5217 – 5221; *Angew. Chem. Int. Ed.* **2010**, *49*, 5091 – 5095.

[6] M. Reiher, O. Salomon, B. A. Hess, *Theor. Chem. Acc.* **2001**, *107*, 48 – 55.

[7] a) D. Janardanan, Y. Wang, P. Schyman, L. Que, Jr., S. Shaik, *Angew. Chem.* **2010**, *122*, 3414 – 3417; *Angew. Chem. Int. Ed.* **2010**, *49*, 3342 – 3345; b) S. Shaik, H. Chen, D. Janardanan, *Nat. Chem.* **2011**, *3*, 19 – 27; c) H. Hirao, D. Kumar, L. Que, Jr., S. Shaik, *J. Am. Chem. Soc.* **2006**, *128*, 8590 – 8606; d) For a similar statement, see: L. Bernasconi, M. J. Louwerse, E. J. Baerends, *Eur. J. Inorg. Chem.* **2007**, 3023 – 3033.

[8] a) Jaguar, version 7.6; Schrödinger, LLC: New York, **2008**; b) Gaussian03 (Revision D.01), M. J. Frisch, et al. Gaussian, Inc., Wallingford, CT, **2004**. See the Supporting Information for full citation of G03.

[9] A. Altun, W. Thiel, *J. Phys. Chem. B* **2005**, *109*, 1268 – 1280.

[10] R. Poli, J. N. Harvey, *Chem. Soc. Rev.* **2003**, *32*, 1 – 8.

[11] a) R. P. Bell, *Proc. R. Soc. London Ser. A* **1936**, *154*, 414 – 421; b) M. G. Evans, M. Polanyi, *Trans. Faraday. Soc.* **1938**, *34*, 11 – 24.

[12] D. Schröder, S. Shaik, *Angew. Chem.* **2011**, *123*, 3934 – 3935; *Angew. Chem. Int. Ed.* **2011**, *50*, 3850 – 3851.

[13] a) H. Hirao, D. Kumar, W. Thiel, S. Shaik, *J. Am. Chem. Soc.* **2005**, *127*, 13007 – 13018; b) D. Janardanan, D. Usharani, H. Chen, S. Shaik, *J. Phys. Chem. Lett.* **2011**, *2*, 2610 – 2617.

[14] E. Carter, W. A. Goddard III, *J. Phys. Chem.* **1988**, *92*, 5679 – 5683.

[15] a) K. Kitaura, K. Morokuma, *Int. J. Quantum Chem.* **1976**, *10*, 325 – 340; b) D. H. Ess, K. N. Houk, *J. Am. Chem. Soc.* **2008**, *130*, 10187 – 10198; c) W.-J. van Zeist, F. M. Bickelhaupt, *Org. Biomol. Chem.* **2010**, *8*, 3118 – 3127.

[16] a) Z. Gross, G. Golubkov, L. Simkhovich, *Angew. Chem.* **2000**, *112*, 4211 – 4213; *Angew. Chem. Int. Ed.* **2000**, *39*, 4045 – 4047; b) A. Kumar, I. Goldberg, M. Botoshansky, Y. Buchman, Z. Gross, *J. Am. Chem. Soc.* **2010**, *132*, 15233 – 15245.

[17] S. Shaik, W. Z. Lai, H. Chen, Y. Wang, *Acc. Chem. Res.* **2010**, *43*, 1154 – 1165.

[18] a) C. V. Sastri, J. Lee, K. Oh, Y. J. Lee, J. Lee, T. A. Jackson, K. Ray, H. Hirao, W. Shin, J. A. Halfen, J. Kim, L. Que, Jr., S. Shaik, W. Nam, *Proc. Natl. Acad. Sci. USA* **2007**, *104*, 19181 – 19186; b) Y. Kang, H. Chen, J. Y. Jeong, W. Z. Lai, E. H. Bae, S. Shaik, W. Nam, *Chem. Eur. J.* **2009**, *15*, 10039 – 10046.

[19] For other ligand-dependent spin-state reactivity effects, see: L. Kaustov, M. E. Tal, A. I. Shames, Z. Gross, *Inorg. Chem.* **1997**, *36*, 3503 – 3511.

